

Supporting Information

A highly efficient atomic nickel catalyst for CO₂ electroreduction in acidic conditions

Qiao Wu,^{a,b} Jun Liang,^{b,e} Li-Li Han,^b Yuan-Biao Huang,^{b,c,d} Rong Cao,^{a,b,c,d*}*

^aDepartment of Chemistry, College of Chemistry and Chemical Engineering, Xiamen University, Xiamen 361005, China

^bState Key Laboratory of Structural Chemistry, Fujian Institute of Research on the Structure of Matter, Chinese Academy of Sciences, Fuzhou 350002, China

^cUniversity of Chinese Academy of Sciences, Beijing 100049, China

^dFujian Science & Technology Innovation Laboratory for Optoelectronic Information of China Fuzhou, Fujian, 350108, China

^eSchool of Chemical Engineering and Technology, Hebei University of Technology, Tianjin 300401, China

Content

S1. Materials and characterization methods.....	S2
S2. Electrochemical measurements.....	S4
S4. Supporting Figures and Tables.....	S6
S5. References.....	S13

S1. Materials and characterization methods

Materials

All reagents were purchased from commercial sources without further purification. 5, 10, 15, 20-tetra(4-(imidazol-1-yl)phenyl)porphyrindine (TIPP, 97%) was purchased from jinanhenghua. LION Ketjenblack (ECP600JD). NiCl₂·6H₂O, ethyl alcohol, HCl were purchased from Sinopharm Chemical Reagent Co., Ltd.,

Synthesis of Ni-SAC-X (X = 800 °C, 900 °C, 1000 °C)

Synthesis of Ni-SAC-800

Typically, 13.1 mg TIPP dissolved and 3.56 mg NiCl₂·6H₂O were dissolved in 10 mL ethanol after sonicated one hours, 50 mg carbon blacks (Ketjenblack) was dissolved in 30 mL ethanol. The mixture was alternately sonicated and stirred for ten hours. Then, the resulting slurry was heated in an oil-bath at 60 °C under continuous magnetic stirring until the solvent evaporated completely, yielding a black solid. The black solid obtained was ground with a mortar and pestle for 10 min, then transferred into a ceramic crucible and heated up in a tube furnace to 800 °C for 2 hours under a gas flow of 50 standard cubic centimeters per minute (sccm) Ar, obtaining the final products Ni-SAC-800. Inductively coupled plasma atomic emission spectroscopy (ICP-AES) analysis revealed that the content of Ni was 1.19 wt%.

Synthesis of Ni-SAC-900 and Ni-SAC-1000

Ni-SAC-900 and Ni-SAC-1000 were prepared under similar conditions as that of Ni-SAC-800. Impurities of Ni NPs were subsequently removed with 1 M hydrochloric acid in Ni-SAC-900 and Ni-SAC-1000. ICP-AES analysis revealed that the content of Ni were 0.80 wt% in Ni-SAC-900 and 0.554 wt% in Ni-SAC-1000.

Synthesis of NC-800

NC-800 were prepared under similar conditions as that of Ni-SAC-800 without NiCl₂·6H₂O.

S1.2 Characterization methods

Powder X-ray diffraction (PXRD) patterns were recorded on a Miniflex 600 diffractometer using Cu K α radiation ($\lambda = 0.154\text{nm}$). Transmission electron microscope (TEM) images were taken on a FEI TECNAI G2 F20 microscope equipped EDS detector at an accelerating voltage of 200 kV. Before TEM test, the sample was dispersed in ethanol, dropped on the copper net and dried. Aberration-corrected high-angle annular dark-field scanning transmission electron microscopy (AC-HAADF-STEM) measurements were taken on JEM-ARM300F at an accelerating voltage of 300 kV. N₂ adsorption-desorption isotherm and the Brunauer-Emmett-Teller (BET) surface area measurements were measured by using Micromeritics ASAP 2460 instrument. CO₂ adsorption-desorption isotherms were measured by using Micromeritics ASAP 2020 instrument. The content of metals were detected by inductively coupled plasma atomic emission spectroscopy (ICP-AES) on an Ultima2 analyzer (Jobin Yvon). X-ray photoelectron spectroscopy (XPS) measurements were performed on an ESCALAB 250Xi X-ray photoelectron spectrometer (Thermo Fisher) using an Al Ka source (15 kV, 10 mA). The C1s line at 284.8 eV from adventitious carbon was used for energy referencing. Raman spectra were recorded on a Labram HR Evolution microscope with a laser excitation wavelength of 532 nm. The gas chromatography measurements were performed on the Agilent 7820A gas chromatograph (GC) equipped with FID and TCD.

S2. Electrochemical measurements

Electrochemical Measurements was performed in a flow cell using constant current electrolysis method. The flow cell contained a gas–diffusion layer (CeTech GDL280), cation exchange membrane (Nafion–117), Pt electrodes (1.0×3.0 cm²), and an Ag/AgCl electrode. The working electrodes were prepared by drop–casting catalyst ink onto the GDL to reach a total mass loading of ~1 mg cm⁻². The phosphoric acid electrolyte (0.5 M H₃PO₄, 0.5 M KH₂PO₄, and 1.5 M KCl, pH = 2) as the catholyte, 0.5 M H₂SO₄ as the anolyte. The electrolytes were separately circulated compartments using circulating peristaltic pumps at flow rates of 5 mL min⁻¹. CO₂ gas was directly fed to the cathodic GDE at a rate of 30 sccm. The gas phase composition was analyzed by gas chromatograph (Agilent 7820A). The separated gas products were analyzed by a thermal conductivity detector (for H₂) and a flame ionization detector (for CO). All the electrode potentials were measured against the Ag/AgCl electrode without iR compensation and measured potentials were converted to reversible hydrogen electrode (RHE) scale using the following equation:

$$E_{(\text{vs. RHE})} = E_{(\text{vs. Ag/AgCl})} + 0.059 \text{ pH} + 0.197 \text{ V}$$

All electrochemical measurements in this work are at room temperature (298 K, 1 bar).

The Faraday efficiency of a certain gas product was calculated based on the following equations:

$$FE = \frac{PV}{TR} \times \frac{vNF \times 10^{-6} (\text{m}^3/\text{mL})}{I \times 60 (\text{s}/\text{min})}$$

v (vol %): volume concentration of certain gas product in the exhaust gas from the cell (GC data);

V: gas flow rate measured by a flow meter, 30 mL min⁻¹;

I: total steady–state cell current;

N: the electron transfer number for product formation;

F: Faradaic constant, 96485 C mol⁻¹;

R: universal gas constant, 8.314 J mol⁻¹ K⁻¹;

P: one atmosphere, 1.013 × 10⁵ Pa;

T: room temperature, 298.15 K.

Evaluation of turnover frequency (TOF):

$$TOF = \frac{J_{tot} \times FE_{CO}}{NF \times n_{tot}}$$

J_{tot} is recorded current, FE_{CO} is faradaic efficiency of CO, F is the Faraday constant of 96485 C mol^{-1} , n_{tot} is the total amount of Ni on the working electrode, N is the number of electron transferred for product formation, in which it is 2 for CO.

The single pass carbon efficiency (SPCE) of CO_2 towards each product or a group of products was determined using this equation at 298 K, 1 atm:

$$\text{SPCE} = (j \times 60 \text{ sec}) / (N \times F) \div (\text{flow rate (L/min)} \times 1 \text{ (min)}) / (24.05 \text{ (L/mol)})$$

where j is the partial current density of specific group of products from CO_2 reduction, N is the electron transfer for every product molecule.

S3. Figures and Tables:

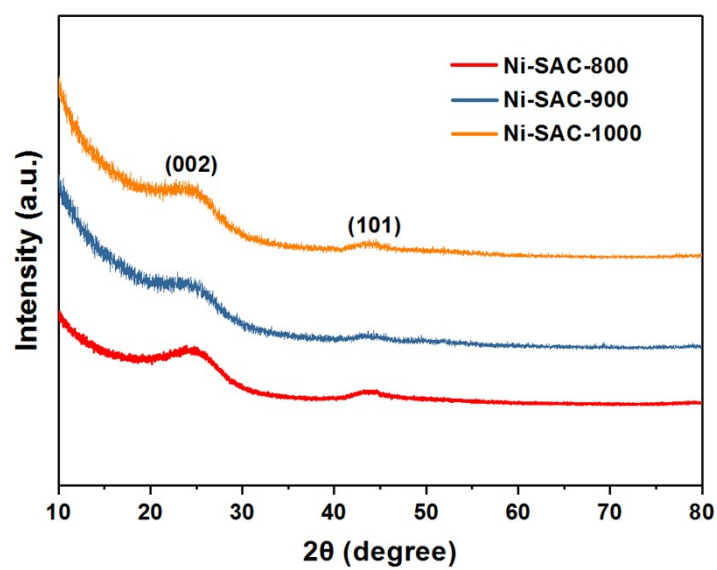


Figure S1. PXRD patterns of Ni-SAC-X (X = 800, 900, 1000).

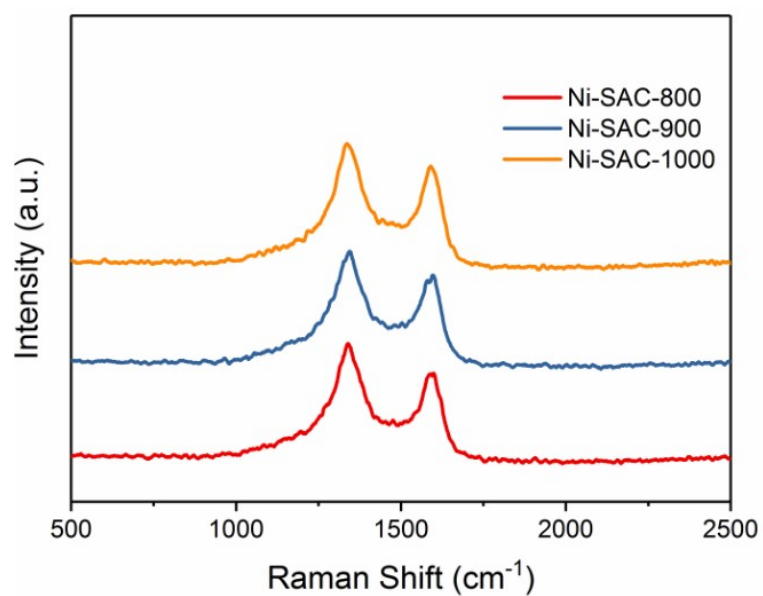


Figure S2. Raman spectra of Ni-SAC-X (X = 800, 900, 1000).

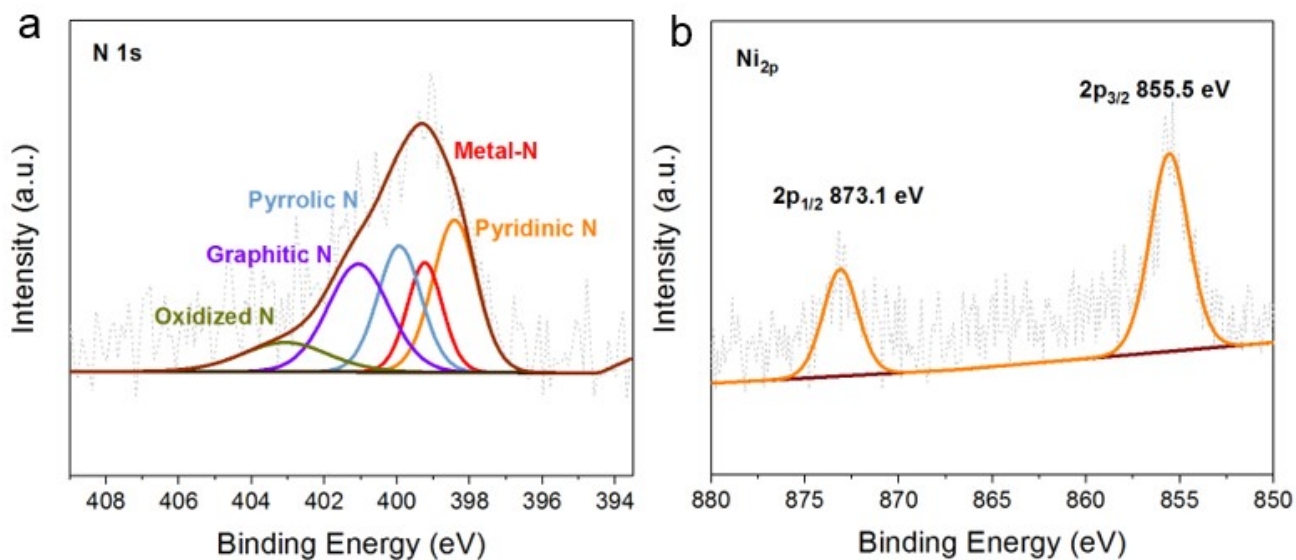


Figure S3. (a) N 1s XPS spectrum of Ni-SAC-800. (b) Ni 2p XPS spectrum of Ni-SAC-800.

The N content of Ni-SAC-800 is 2.18 wt% based on elemental analysis.

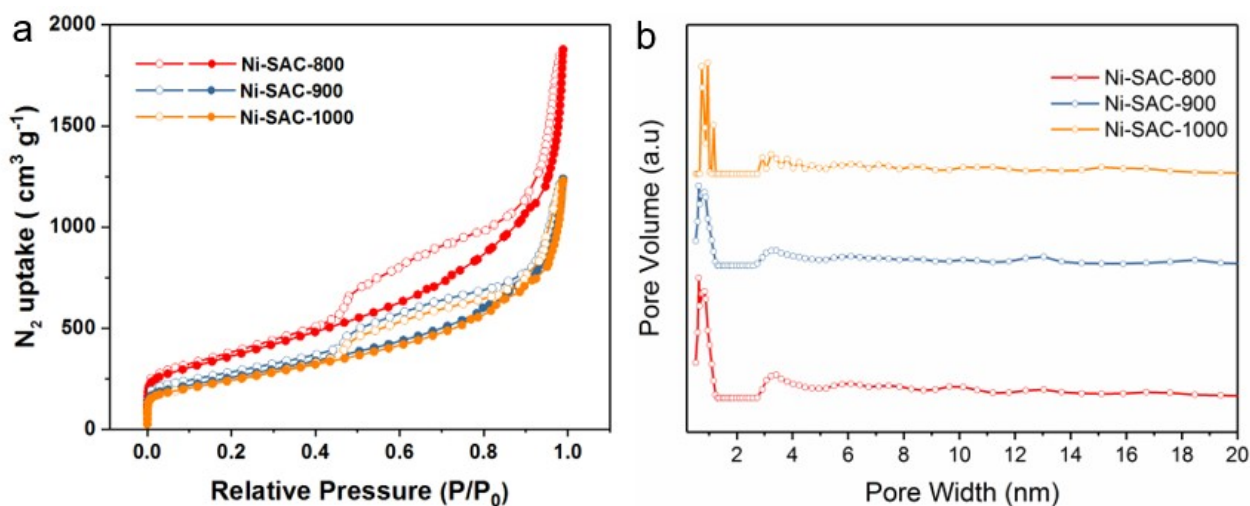


Figure S4. (a) N₂ adsorption–desorption isotherms at 77 K and (b) The pore size distribution (PSD) profile of Ni-SAC-X (X = 800, 900, 1000) based on NL-DFT method.

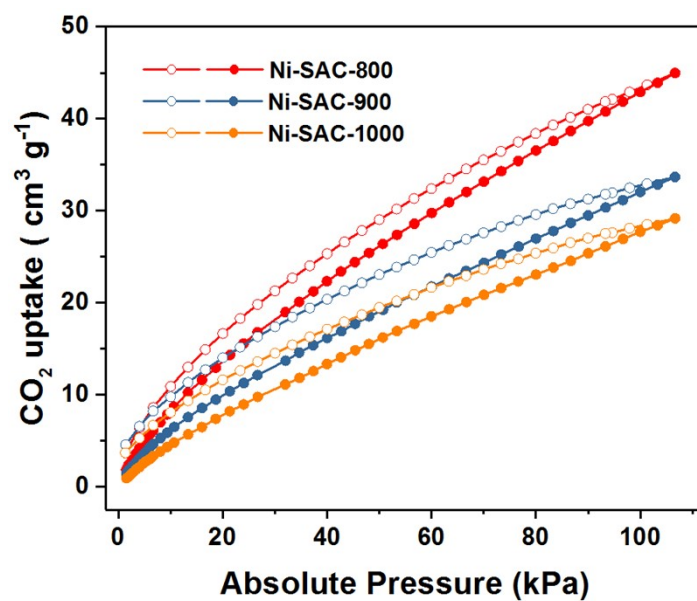


Figure S5. CO₂ adsorption–desorption isotherms at 298 K of Ni–SAC–X (X=800, 900, 1000).

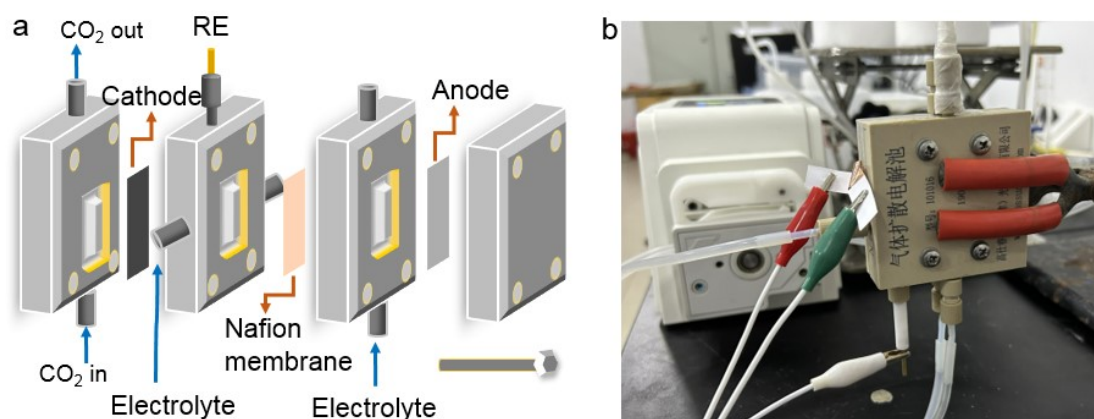


Figure S6. (a) Schematic of a flow cell. (b) Optical photograph of CO₂RR test in flow cell.

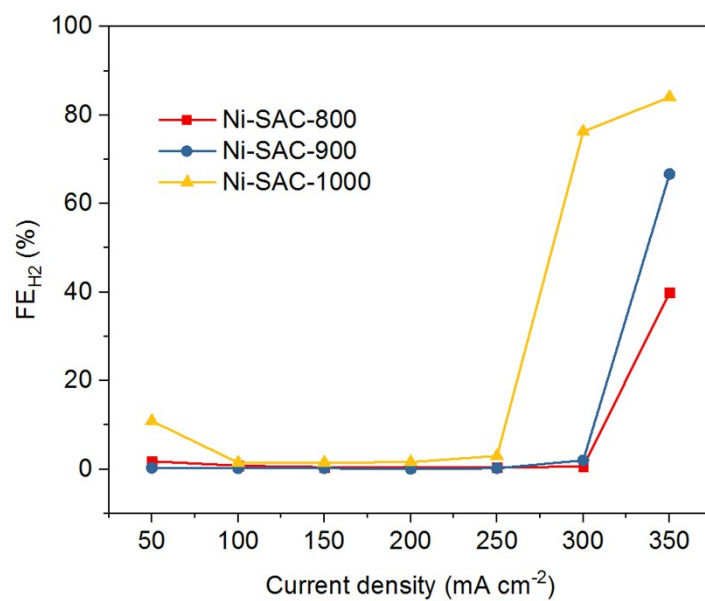


Figure S7. FE_{H₂} of Ni-SAC-X (X = 800, 900, 1000).

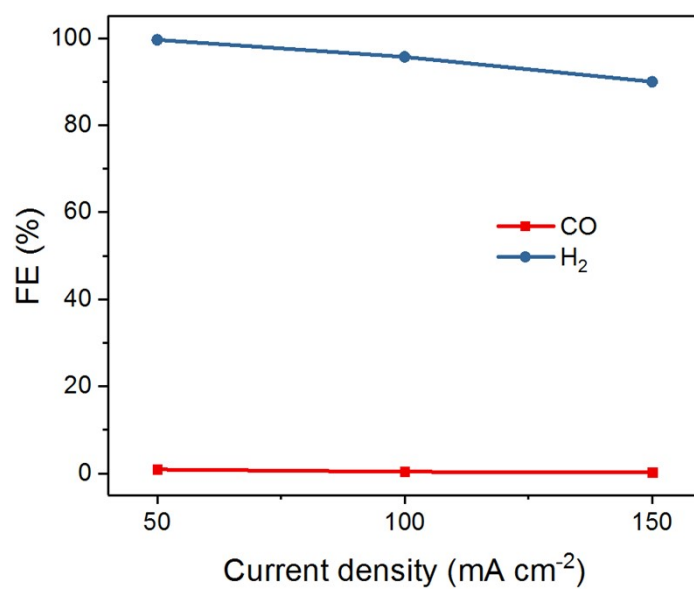


Figure S8. The faradaic efficiency (FE_{CO}) of NC-800 in acidic electrolyte (0.5 M H₃PO₄, 0.5 M KH₂PO₄, and 1.5 M KCl, pH = 2).

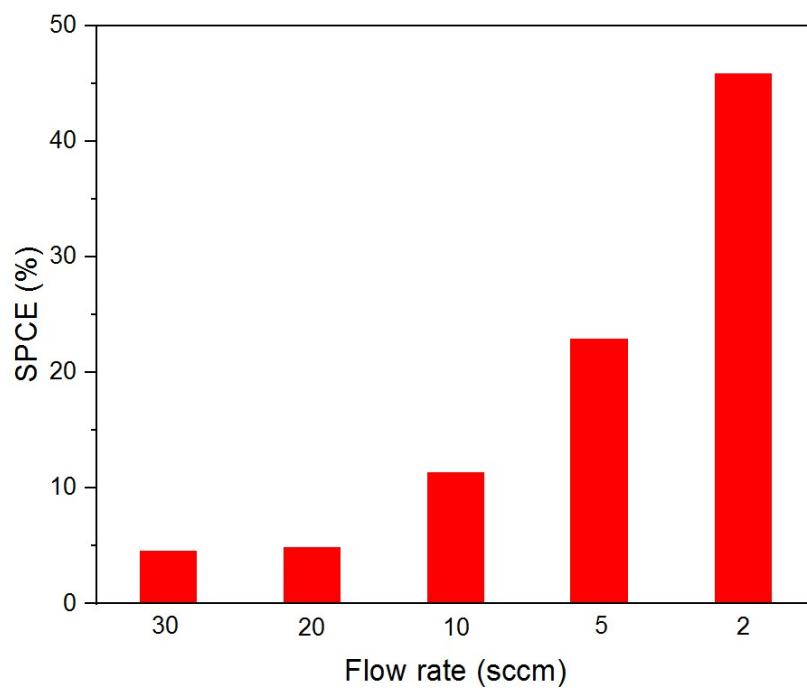


Figure S9. Single pass carbon efficiency in acidic electrolyte (pH = 2) in a flow cell with different CO₂ inflow.

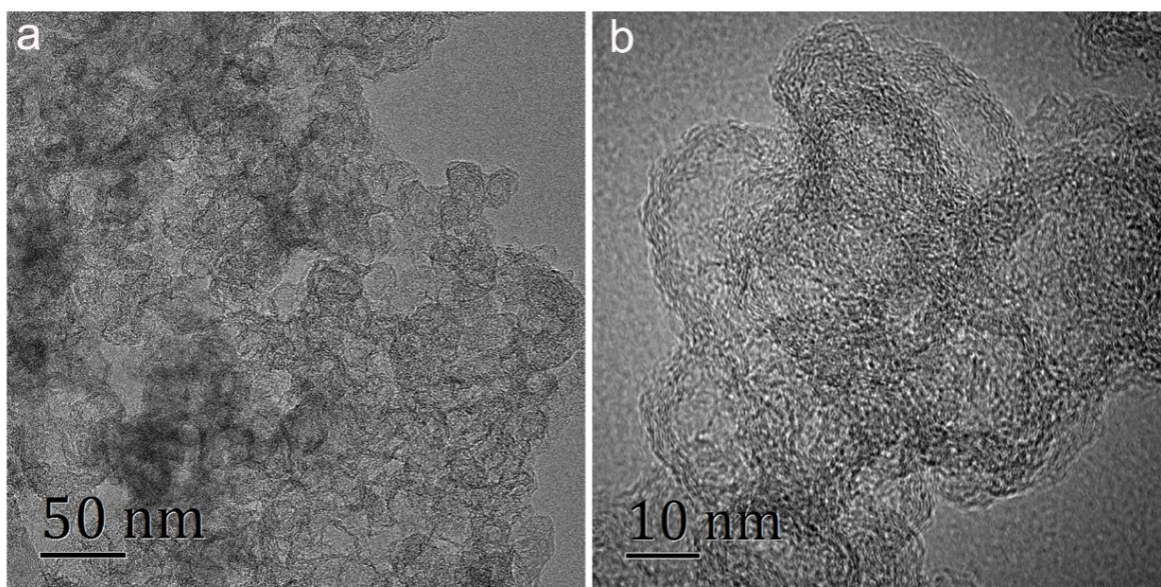


Figure S10. TEM images of Ni-SAC-800 with different scale bar after CO₂RR test in acidic media.

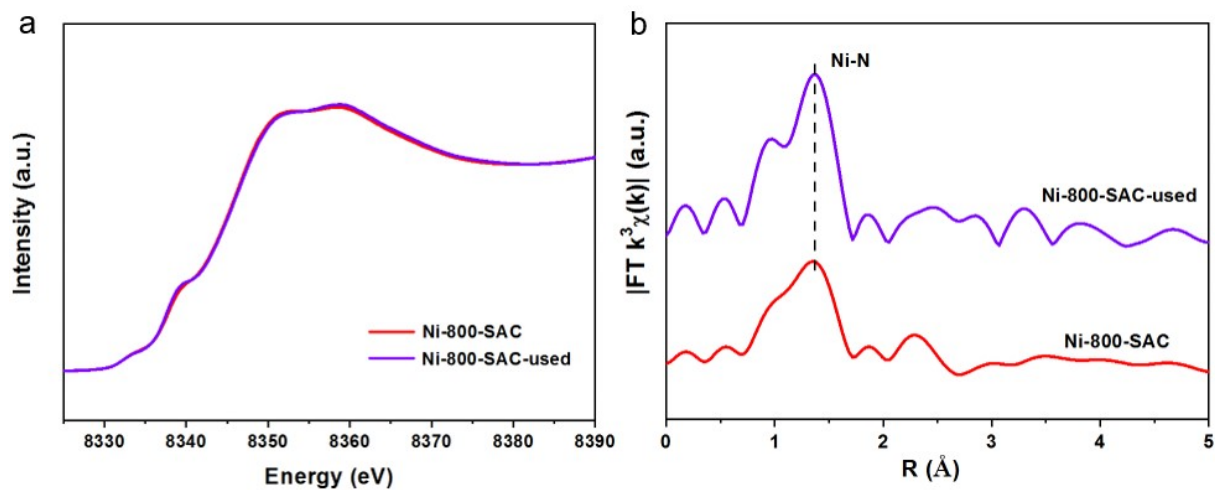


Figure S11. (a) Normalized Ni K-edge XANES spectra and (b) Fourier transform EXAFS spectra for Ni-SAC-800 and after CO₂RR test of Ni-SAC-800-used.

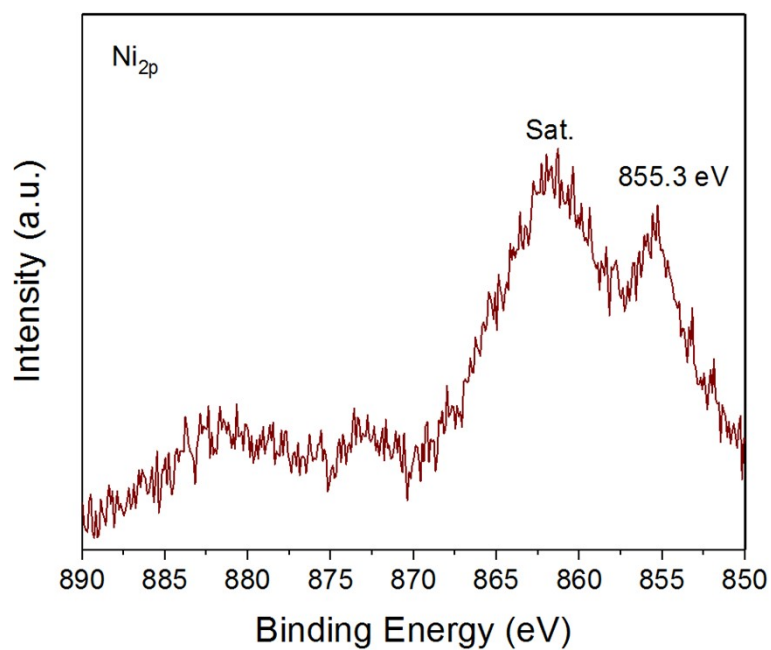


Figure S12. Ni 2p XPS spectrum of Ni-SAC-800 after electrocatalysis.

Table S1. The EXAFS data fitting results of Ni-SAC-800.

Sample	Path	N	R(\AA)	$\sigma^2(10^{-3}\text{\AA}^2)$	$\Delta E_0(\text{eV})$	R factor
Ni-SAC-800	Ni-N	4.1	1.87	6.9	8.8	0.001

Note: N is the coordination number; R is interatomic distance (the bond length between central atoms and surrounding coordination atoms); σ^2 is Debye–Waller factor (a measure of thermal and static disorder in absorber–scatterer distances); ΔE_0 is edge–energy shift; R factor is used to value the goodness of the fitting.

Table S2. Comparison of acidic electrochemical CO₂ reduction with other recent reports. Only reports with pH \leq 4.2 were compared.

Catalysts	pH	FE _{CO} (%)	J_{CO} (mA cm ⁻²)	Ref.
Ni-SAC-800	2.0	99.9	296.4	This work
Polycrystalline Au	3.0	90 ^a	–	1
Ni ₃ N/MCNT	2.5	50.1	–	2
Ni ₅ @NCN	2.5	80	102	3
Au	4	90	100	4
Co–P4VP	2.6	92	2.1	5
Co:P4VP	2.6	92	78.2	6
Au/C	1.5	91	125 ^a	7
CoPP–PG	3	60.3	0.44	8
Ag iRDE	4.17	96.8	2.6	9

^aEstimated value.

S5. References

- [S1] C. J. Bondue, M. Graf, A. Goyal, M. T. M. Koper, *J. Am. Chem. Soc.* **2021**, *143*, 279–285.
- [S2] Z. Wang, P. F. Hou, Y. L. Wang, X. Xiang, P. Kang, *ACS Sustainable Chem. Eng.* **2019**, *7*, 6106–6112.
- [S3] Z. Liu, T. Yan, H. Shi, H. Pan, Y. Cheng and P. Kang, *ACS Appl. Mater. Inter.* **2022**, *14*, 7900–7908.
- [S4] M. C. O. Monteiro, M. F. Philips, K. J. P. Schouten, M. T. M. Koper, *Nat. Commun.* **2021**, *12*, 4943.
- [S5] Y. S. Liu, C. C.L. McCrory, *Nat. Commun.*, **2019**, *10*, 1683.
- [S6] N. Fujinuma, A. Ikoma, S. E. Lofland, *Adv. Energy Mater.* **2020**, *10*, 2001645.
- [S7] J. Gu, S. Liu, W. Y. Ni, W. H. Ren, S. Haussener, X. L. Hu, *Nat. Catal.* **2022**, *5*, 268–276.
- [S8] J. Shen, R. Kortlever, R. Kas, Y. Y. Birdja, O. Diaz–Morales, Y. Kwon, I. Ledezma–Yanez, K. J. P. Schouten, G. Mul, M. T. M. Koper, *Nat Commun.* **2015**, *6*, 8177.
- [S9] P. Moreno–García, N. Kovacs, V. Grozovski, M. D. J. Galvez–Vazquez, S. Vesztergom, P. Broekmann, *Anal. Chem.* **2020**, *92*, 4301–4308.